

SURFACE PLASMONIC EFFECT IN HIGHLY DOPED SEMICONDUCTOR NANOCRYSTALS, A POTENT OVERVIEW

Dr. Manas Saha Department of Physics, Shibpur Dinobundhoo Institution (College), 412/1 G.T Road (south), Howrah-711102, West Bengal, India. Mail: idformanas2@gmail.com

Semiconductor nanocrystal exhibit localized surface plasmon resonance phenomena depending upon aliovalent element doping in as synthesized nanocrystals. Now in recent time aliovalent doped degenerate semiconductor nanocrystals (NCs) are addressed considerable attention for localized surface plasmon resonance (LSPRs) absorption, optical bandgap enhancing, multiple emission centers and high carrier concentration with excellent visible light transparency. The collective oscillation of free electrons in metals leads to plasmon effect on the surface of metals. The frequency of oscillation depends on the concentration of free electrons and the dielectric constant of metal. The interaction of light with high dense electron gives rise to absorption due to plasmonic phenomenon. The optical absorption frequency can be easily varied from the ultraviolet (UV) to far-infrared (FIR) region through the reduction of size of metals. High electrical conductivity of metal limits the plasmonic resonance application due to high absorption loss. Low loss plasmonic materials are very attractive because of development new technology such as photothermal therapy, surface plasmon resonance sensor, plasmon enhanced fluorescence and solar cell. It is found that doped semiconductor nanocrystals reveal plasmonic effect in near infrared (NIR) region through the introduction of more carrier concentration in the conduction band of wide band gap semiconductor. Cation and anion vacancies and doping by suitable atoms enhance the carrier concentration of semiconductor. Wide band gap semiconductors possess high optical transparency in the visible region and can have high electrical conductivity due to excess charge carrier in conduction band. Thus heavily doped semiconductors with large band gap may have the combined property of high optical transparency, good electrical conductivity and moderate plasmonic absorption.

1. Surface plasmon

Surface plasmon resonance (SPR) exploits the coherent electron oscillations that are driven at

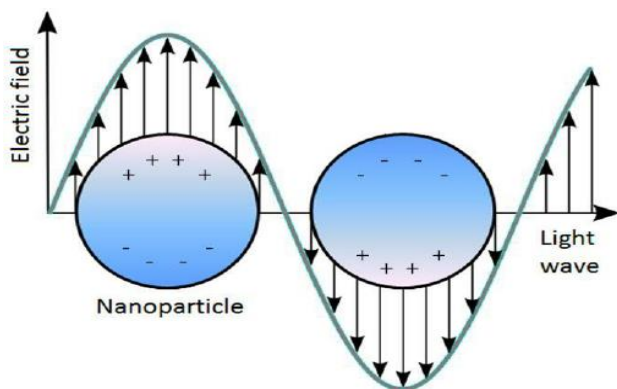


Figure1: Schematic presentation of the collective oscillation of electrons in metal nanoparticles by excitation of electromagnetic wave.

the frequency of the incident electromagnetic field.¹⁻² Electric component of electromagnetic wave vector excites free electrons to have collective oscillation shown in Figure 1. Collective oscillation results in propagation of electromagnetic surface mode at the interface of metal and surrounding dielectric medium.³ Surface plasmon resonance addresses couplings of electromagnetic field to the kinetic motion of free charge carriers. Indeed the challenge is plasmonic propagation loss. While presence of negative real part of permittivity in noble metal causes sub wavelength confinement and also have significant large imaginary component of permittivity results in long range plasmonic propagation loss.⁴ So it is needed a material which allows sub wavelength optical

confinement and loss mitigation simultaneously. Figure 2 demonstrates the classification of materials on the basis of two important parameters that determine the optical properties of conducting materials: the carrier density and carrier mobility. Higher carrier mobilities interpret to lower material losses. From Figure 2 it is convenient that degenerately doped semiconductors are best conductive plasmonic material.

Different types of chemical doping viz. aliovalent substitution doping in oxide semiconductor (mainly transparent conducting oxide (TCO)),⁵⁻⁷ vacancy doping and interstitial doping results excess charge carrier density.⁸ In nanoscale regime surface plasmon resonance is resulting as localized surface plasmon resonance (LSPR). Excellent achievement in colloidal synthesis of nano TCO material soundly improves the tunability of LSPR. Excitation of LSPR in nanocrystals (NCs) results in strong optical absorption, scattering and strong electromagnetic near field enhancement around the nanocrystals⁹ those can be tuned in a wide range of optical spectrum from visible to far infrared region by tuning dopant concentration, post synthetically treatment¹⁰⁻¹¹ via chemical oxidation reduction,¹² electrochemical,¹³ and photochemical control.¹⁴ Due to remarkable optical absorption, scattering and strong electromagnetic near field enhancement utilize in molecular-specific imaging and sensing, photo-diagnostics, and selective photothermal therapy.

2. Theory of surface Plasmon:

The charge carriers are displaced by incoming electromagnetic energy with respect to the nuclei in noble nano metal. Excitation of LSPR by a coherent electric field creates a resonance at a particular wavelength and results in strong surface plasmon absorption band, intense light scattering and an enhancement of coherent electromagnetic field.

SPR can be tuned in doped semiconductor by the variation of aliovalent dopant concentration, nanoparticles size, shape and surrounding dielectric medium. Conventional noble metals such as gold, silver and platinum can exhibit LSPR from visible to NIR region. In consequence of noble metal some TCO material lead to plasmon resonance in NIR and MIR due to lower quantized plasma energy.¹⁵⁻¹⁶ Both plasmon absorption band intensity and energy are correlated to free carrier concentration in TCO NCs that can be quantitatively described by Drude-Lorentz theory. The surface plasmon energy has two decay channels. One channel is manifested by scattering-loss spectra and other is absorption band cross section.¹⁷ So the total extinction cross section is sum of scattering cross

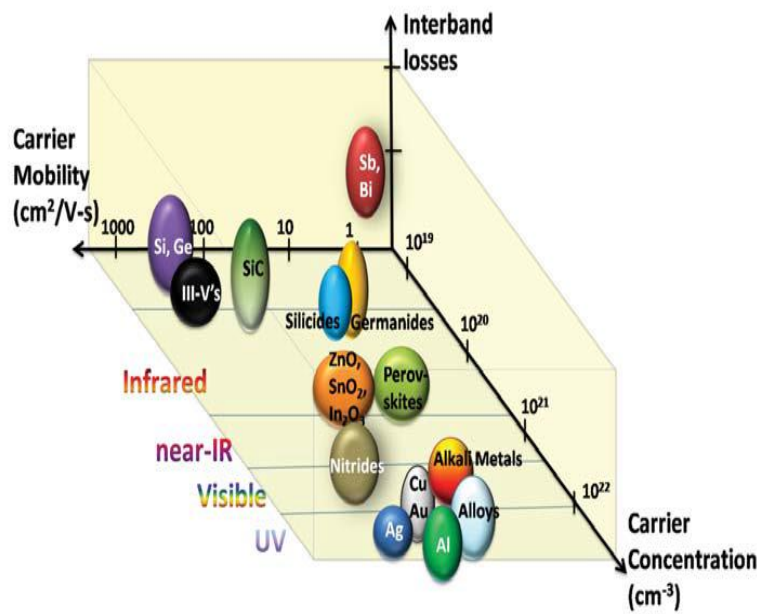


Figure 2: Conclude oxide semiconductor maintain optimum carrier concentration, mitigation loss and carrier mobility.

section (C_{sca}) and absorption cross section (C_{abs}) can be written as:

$$C_{ext} = C_{abs} + C_{sca} \tag{1}$$

Extinction is totally depended on the polarizability(α) of the nanoparticles. i.e. it includes the dielectric function of metal.¹⁷

3. Drude Theory

Drude explained the thermal as well as electrical property of metals by kinetic gas theory.¹⁸⁻¹⁹ Since he considered electrons are moving freely between collisions or elastic scattering with lattice defect or phonons. Here Arnold Sommerfeld modified the idea of Drude and he adopt that electronic and optical properties are determined by conduction band electrons only.²⁰ Now the excitation of metal by external electric field is described by Drude-Lorentz-Sommerfeld model. The optical properties of

metal are evaluated (a) by the fact that conduction electrons can move freely within the bulk of material and (b) inter band excitation can be possible if the energy of electromagnetic wave exceeds the band gap energy of the respective material. In real scenario presence of electric field leads to a displacement r of an electron which is associated with a dipole moment μ of metal according to $\mu = er$. Here displacement of electron is bound by positive ion core which leads to Coulomb attraction acting as a restoring force for the electrons. Macroscopic effect in optical and electrical properties is ascribed by cumulative effect of each single electron in conduction band. Since the macroscopic polarization per unit volume $P = n\mu$, where n is the number of electrons per unit volume. Now the electric displacement D is related to this macroscopic polarization by

$$\mathbf{D}(\mathbf{r}, t) = \epsilon_0 \mathbf{E}(\mathbf{r}, t) + \mathbf{P}(\mathbf{r}, t) \quad (2)$$

We also have from electro statistic

$$\mathbf{D} = \epsilon_0 \epsilon \mathbf{E} \quad (3)$$

Combine equation 2 and 3 by assuming isotropic medium, the dielectric constant can be expressed as^{18, 21-22}

$$\epsilon = 1 + \frac{|P|}{\epsilon_0 |E|} \quad (4)$$

Amount of displacement r and macroscopic polarization \mathbf{P} can be found out by solving the equation of motion of the electrons that are perturbed by an external electromagnetic field. While in case of bulk metal damping constant (γ) is proportional to the Fermi velocity v_F and inversely proportional to the bulk mean free path l_∞ ($\gamma = v_F/l_\infty$). At a starting point we can consider the electric field of an electromagnetic wave travelling in X direction with propagation direction along Z axis. Now we consider that

$$\bar{E}_z = \bar{E}_0 e^{i\omega t} \quad (5)$$

By applying Drude-Sommerfeld model equation of motion of an electron with mass m_e and charge e is governed by

$$m_e \frac{\partial^2 x}{\partial t^2} + m_e \gamma \frac{\partial x}{\partial t} + m_e \omega_0^2 x = -e \bar{E}_0 e^{i\omega t} \quad (6)$$

Where E_0 , ω and ω_0 are the amplitude, the frequency of the applied electric field and induced frequency of oscillating electron. The solution of equation (6) is¹⁷⁻²⁰

$$x(t) = -\frac{e}{m_e} \frac{1}{(\omega_0^2 - \omega^2 - i\gamma\omega)} \bar{E}_0 e^{i\omega t} \quad (7)$$

Microscopic dipole moment P is connected to the polarization p with carrier density n in conduction band by

$$P = n.p = -n.e.x \quad (8)$$

By combining equation (4), (7) and (8) leads to

$$\epsilon(\omega) = 1 + \frac{ne^2}{\epsilon_0 m_e} \frac{1}{(\omega_0^2 - \omega^2 - i\gamma\omega)} = 1 - \frac{ne^2}{\epsilon_0 m_e} \frac{\omega_p^2}{(\omega_0^2 - \omega^2 - i\gamma\omega)} \quad (9)$$

Where

$$\omega_p^2 = \frac{ne^2}{\epsilon_0 m_e} \quad (10)$$

ω_p is the volume plasma frequency with vacuum permittivity ϵ_0 . In lattice environment scenario it might be change m_e by m^* , the lattice electron effective mass. Finally the frequency dependent dielectric function can be expressed as:¹⁸

$$\epsilon(\omega) = \epsilon'(\omega) + i\epsilon''(\omega) = 1 + \omega_p^2 \frac{(\omega_0^2 - \omega^2)}{(\omega_0^2 - \omega^2)^2 + \gamma^2 \omega^2} + i\omega_p^2 \frac{\gamma\omega}{(\omega_0^2 - \omega^2)^2 + \gamma^2 \omega^2} \quad (11)$$

In conduction band scattering of electrons with electrons ($e-e$), lattice defect ($e-d$) and phonon ($e-p$) results in damping of collective oscillation. At free electron theory damping constant is depicted by the inverse of the scattering time of the electron:¹⁷

$$\gamma = \tau^{-1} = \tau_{e-e}^{-1} + \tau_{e-d}^{-1} + \tau_{e-ph}^{-1} \quad (12)$$

For the bulk electron-phonon term is denominating one hence γ should be a constant. In case of small particles due to size reduction surface acts as an additional scatter where mean free path of electrons becomes comparable to the size of particles. In nano dimension these interactions of the conduction electrons with particle surface dominate which result in a reduced effective mean free path

of electrons. According to Drude model²³ the damping constant γ can be expressed as in term of particle radius such as :

$$\gamma(R) = \gamma_0 + \frac{A.v_F}{R} \quad (13)$$

Where γ_0 is the bulk damping constant v_F is the velocity of the conduction electrons at the Fermi energy, and A includes details of the scattering processes.²³

4. Mie Theory

The breakthrough in understanding of light scattering by spherical metal structures within the frame of electrodynamics was first described by Gustave Mie. in 1908.²⁴ He obtained solution of Maxwell equation by choosing appropriate boundary condition and used multiple expansions of the electric and magnetic field with taking input parameters as particle size and optical material functions of the particle and the surrounding medium. It is possible by Mie theory to get an understanding of light scattering by structures with other regular shapes, such as cylinders with arbitrary radius and ellipsoids with any size.¹⁷ Now for the particles much smaller than the incoming electromagnetic effect *i.e.*, $R \ll \lambda$ then cross-sections for scattering, extinction and absorption can be expressed as:¹⁷

$$C_{ext}^{Mie} = \frac{2\pi}{k^2} \sum (2n+1) \text{Re}(a_L + b_L) \quad (14)$$

$$C_{Sc}^{Mie} = \frac{2\pi}{k^2} \sum (2n+1) \{|a_L|^2 + |b_L|^2\} \quad (15)$$

$$C_{abs}^{Mie} = C_{ext}^{Mie} - C_{Sc}^{Mie} \quad (16)$$

Where $k = \frac{2\pi}{\lambda}$ and a_L and b_L are the scattering cross section coefficient. These are the particle size parameter (α) depended index which are governed by

$$\alpha = \frac{2\pi r}{\lambda} \quad (17)$$

$$a_L = \frac{m\psi(m\alpha)\psi'(\alpha) - \psi_L'(m\alpha)\psi_L(\alpha)}{m\psi(m\alpha)n_L'(\alpha) - \psi_L'(m\alpha)n_L(\alpha)} \quad (18)$$

$$b_L = \frac{\psi_L(m\alpha)\psi_L'(\alpha) - m\psi_L'(m\alpha)\psi_L(\alpha)}{\psi(m\alpha)n_L'(\alpha) - m\psi_L'(m\alpha)n_L(\alpha)} \quad (2.19)$$

Where ψ_L and n_L are represents the Riccati-Bessel functions and prime indicates the first derivative of function. Here $m = \frac{n}{n_m}$, n is a complex number as metallic particle have absorbing and its refractive index n_m is the real refractive index of liquid surrounding medium. Here L is the summation index of admitted the spherical multipole excitations in the particle. In case of small particles for dipole scattering resonance, only the term $l=1$ is applied in Mie theory and other higher order term $l=2$ to quadrupolar fields and so on are neglected. So in dipolar field approximation C_{ext}^{Mie} for spherical particle simplified as:²⁵

$$C_{ext}^{Mie} = \frac{18\pi V \varepsilon_m^{3/2}}{\lambda} \frac{\varepsilon''(\omega)}{(\varepsilon'(\omega) + 2\varepsilon_m)^2 + \varepsilon''^2(\omega)} \quad (20)$$

ε_m is the dielectric constant of surrounding medium, ε_ω is the dielectric constant of spherical particle. V is the volume of spherical particle. C_{ext} has admitted a resonance when $(\varepsilon'(\omega) + 2\varepsilon_m)^2 + \varepsilon''^2(\omega)$ is minimum. When $(\varepsilon''(\omega))$ is also very small then

$$\varepsilon'(\omega) = -2\varepsilon_m \quad (21)$$

at resonance.

5. Influence of dopant concentration on LSPR

In classical Drude model charge carriers are treated as nearly free non-interacting “quasi-particles”, interacting only lattice nuclei, vacancies and dopant ions only through instantaneously collision. This is the basic building block of SPR absorption understanding to the free carrier density. So the LSPR frequency is associated with the charge carrier density in the NCs, as shown in Figure 3. Equation (10) depicts the Drude approximation of the dielectric function of a material with free charge carriers. In equation (10) ω_p is the bulk plasmon frequency, γ is a damping frequency, n is the density of free charge carriers, e is the charge of the electron, ϵ_0 is the vacuum permittivity and m_{eff} is the effective mass of the charge carriers (electrons or holes). In alliovalent doped TCO material free carriers are results in broad LSPR absorption

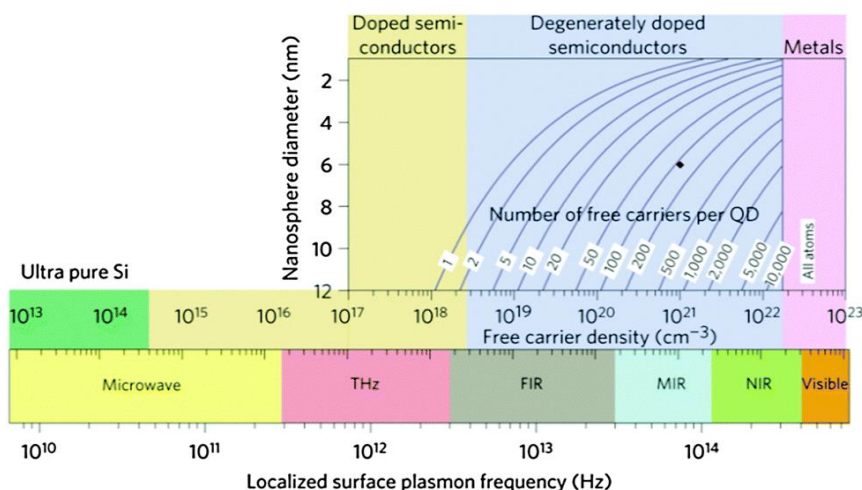


Figure 3: LSPR frequency is associated with the charge carrier density in the NCs.²⁷

6. Influence of nanoparticle size on the LSPR

The total extinction coefficient of small metallic particles is given in Mie’s theory (equation 20). For nanoparticles much smaller than the wavelength of the absorbing light (about 25 nm for gold particles)

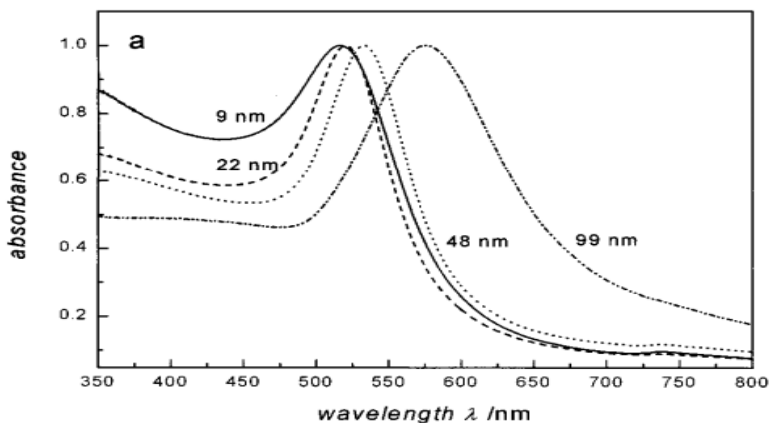


Figure 4: Size effects on the LSPR absorption in spherical gold nanoparticles. The UV-vis absorption spectra of colloidal solutions of gold nanoparticles with diameters

of the conduction electron is larger than the particle radius. In this scenario plasmon resonance will be broadened and red-shifted with decreasing particle size. In this limit the plasmon resonance bandwidth is inversely proportional to the particle radius as from Drude free electron model in equation 13. Hence carriers are scattered elastically from surfaces rapidly, results in incoherence between scattered waves. *S. Link et al.*²⁹ shown size dependence of the plasmon absorption band as depicted in Figure 4.

7. Solvent effect on the LSPR absorption peak

Surrounding medium’s refractive index has correlation on the dielectric function of the material as governed by equation (21). In continuation with equation (21) it is confirmed that have a dependency of the plasmon resonance on the refractive index n of the surrounding medium ($n^2 = \epsilon_m$). Gradual

peak in IR to mid-IR region. Based on Drude theory one can estimate the concentration of free carriers in doped TCO material from LSPR absorption peak and make a correlation with doping amount in pure sample.²⁶⁻²⁷ However, factors including the poly disparity of NCs and non-uniform elemental distribution may restrict the applicability of this simple analysis.²⁸ Here Figure 3 depicts the plasmon absorption band position in energy scale with carrier concentration.

only the dipole term is assumed to contribute to the absorption (dipole approximation).¹⁷ In quasi-static regime where incoming light wavelength much larger than particle size ($R \ll \lambda$) *i.e* electron-surface scattering becomes important. The extinction cross section in Mie theory becomes independent of the particle volume,¹⁷ is contradictory with observations found experimentally for small metallic nanoparticles. As the particle size is reduced that electron scattering at the nanoparticle surface plays an enhanced role in such small particles, as the mean free path

increase of dielectric constant leads to decrease of the Coulombic restoring force of the electron cloud of nanoparticles, those results in decrease of the plasmon frequency. Figure 5 represents the experimental results of solvent variation LSPR absorption peak. A red-shift of the LSPR absorption peak is noticed with increasing refractive index of the solvent. Refractive index sensitivity may be beneficial for biosensing applications.

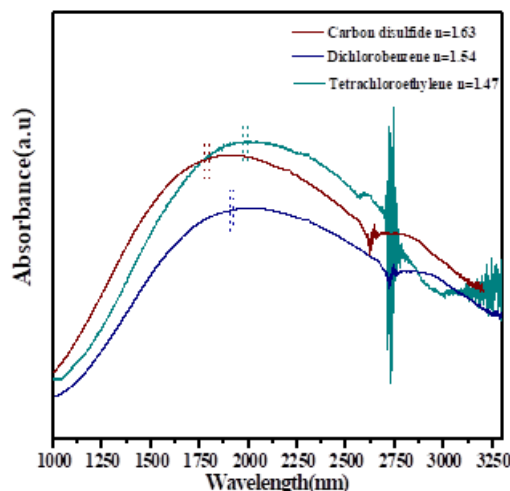


Figure 5: Red-shift of LSPR with increased refractive index.

8. Shape dependency on LSPR absorption

The LSPR absorption wavelength depends on the complex dielectric function of the dielectric function of material, surrounding medium (ϵ_m), and the nanoparticles size and shape. Shape dependent anisotropy has large contribution on LSPR absorption pattern. In Mie approximation the excitation of the LSPR is independent of the polarization of excitation as spherical particle has high symmetry. In quasi-static regime, where $R \ll \lambda$, Mie theory can be extended according to R. Gans. by combining depolarization factors for the three axes of the particle to account for the contribution of the light polarization in different mode for axes of the nanoparticles spectrum. Nanoparticles for arbitrary shapes need to a computational method for solving Maxwell's equations using numerical tools viz. the finite difference in the time domain method (FDTD) boundary element method (BEM) and the discrete dipole approximation (DDA). However for regular shapes like nanorod electromagnetic wave polarization plays an excellent role as two main directions of collective oscillation identified such as along the main axis of the rod or perpendicular to it. Previously reported gold nanorods has showed the extinction spectrum of two bands, corresponding to the oscillations along (longitudinal or L-band) and perpendicular to the long axis (transverse or T-band) of nanorod. Now according to Mie Gans modification extinction cross section (C_{ext}) represented as³⁰

$$C_{ext} = \frac{2\pi V \epsilon_m^{3/2}}{3\lambda} \sum \frac{\left(\frac{1}{P_j^2}\right) \epsilon''(\omega)}{(\epsilon(\omega) + \frac{1-P_j}{P_j} \epsilon_m)^2 + \epsilon''^2(\omega)} \quad (22)$$

P_j are the depolarization factors for the three axes x , y and z for three dimensional system ($j =$

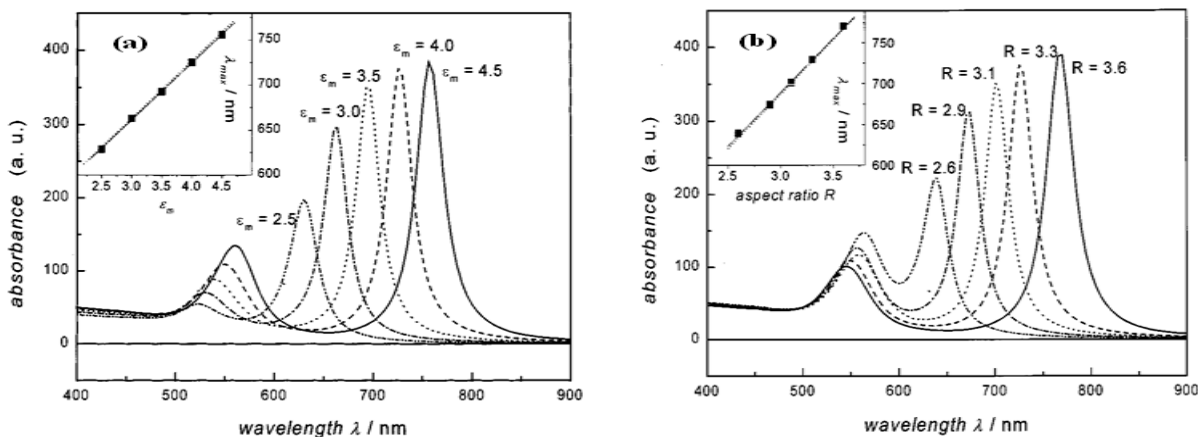


Figure 6: (a) Calculated absorption spectra of elongated ellipsoids with varying medium dielectric constant ϵ_m using eq 22. The aspect ratio was fixed at a value of 3.3. The inset shows a plot of the maximum of the longitudinal plasmon band determined from the calculated spectra as a function of the medium dielectric constant. Adapted from ref.31, copyright 1999, A.C.S (b) Calculated absorption spectra of elongated ellipsoids with varying aspect ratios R using eq. 25. The medium dielectric constant was fixed at a value of 4. The inset shows a plot of the maximum of the longitudinal plasmon band determined from the calculated spectra as a function of the aspect ratio

A , B , and C of the nanoparticle with $A > B = C$). Depolarization factors are represented as ³¹

$$P_x = \frac{1-e^2}{e^2} \left[\frac{1}{2e} \ln \left(\frac{1+e}{1-e} \right) - 1 \right] \quad (23)$$

$$P_y = P_z = \left(\frac{1-P_x}{2} \right) \quad (24)$$

Where e is geometric factor appeared in equation (23) defined as

$$S = \left(1 - \frac{1}{R^2} \right)^2 \quad (25)$$

R is the aspect ratio of nanoparticles. From equation (22) it is clear that two distinct perpendicular bands arise along with the principal long axis band. Multiple plasmonic bands are studied in different aspect ratios for gold nanoparticles using equation 22 (Figure 6).³¹

References:

- (1) L. Novotny and B. Hecht, *Principles of nano-optics*. Cambridge university press, 2012.
- (2) D. R. Smith, J. B. Pendry, and M. C. K. Wiltshire, "Metamaterials and negative refractive index," *Sci.*, vol. 305, no. 5685, pp. 788–792, 2004.
- (3) E. Hutter, J. H. Fendler, *Adv. Mater.* **2004**, 16, 1685-1706.
- (4) W.A. Murray, W. L. Barnes *Adv. Mater.* **2007**, 19, 3771-3782.
- (5) M. Sturaro, E. D. Gaspera, N. Michieli, C. Cantalini, S. M. Emamjomeh, M. Guglielmi, A. Martucci, *ACS Appl. Mater. Interfaces*, **2016**, 8, 30440–30448.
- (6) M. Xi, B. M. Reinbard, *J. Phys. Chem. C* **2018**, 122, 5698–5704.
- (7) S. Ghosh, M. Saha, S. K. De, *Nanoscale* **2014**, 6, 7039-7051.
- (8) A. Agarwal, S. H. Cho, O. Zandi, S. Ghosh, R. W. Johns, D. J. Miliron, *Chem. Rev.* **2018**, 118, 3121–3207.
- (9) G. V. Naik, V. M. Shalaev, A. Boltasseva, *Adv. Mater.* **2013**, 25, 3264-3294.
- (10) I. Kriegel, C. Jiang, J. R.-Fernandez, R. D. Schaller, D. V. Talapin, E. da. Como, J. Feldmann, *J. Am. Chem. Soc.* **2012**, 134, 1583-1590.
- (11) J. M. Luther, P. K. Jain, T. Ewers, A. P. Alivisatos, *Nature Mater.* **2011**, 10, 361-366.
- (12) D. Dorfs, T. Hartling, K. Mistaza, N. C. Bigall, M. R. Kim, A. Genovese, A. Falqui, M. Povia, L. Manna, *J. Am. Chem. Soc.* **2011**, 133, 11175-11180.
- (13) V. B. Llorente, V. M. Dzhagan, N. Gaponik, R. A. Iglesias, D. R. T. Zahn, V. Lesnyak, *J. Phys. Chem. C* **2017**, 121, 18244–18253.
- (14) A. Callegari, D. Tonti, M. Chergui, *Nano Lett.*, **2003**, 3, 1565-1568.
- (15) E. D. Gaspera, M. Bersani, M. Cittadini, M. Guglielmi, D. Pagani, R. Noriega, S. Mehera, A. Salleo, A. Martucci, *J. Am. Chem. Soc.* **2013**, 135, 3439–3448.
- (16) S. Ghosh, M. Saha, V. D. Ashok, B. Dalal, S. K. De, *J. Phys. Chem. C* **2015**, 119, 1180–1187.

- (17) U. Kreibig, M. Vollmer, *Optical Properties of Metal Clusters*, Springer, **2010**.
- (18) S. Hunklinger, *Festkörperphysik*, Oldenbourg Wissensch.Vlg, **2009**.
- (19) I. Kriegel, F. Scotognella, L. Manna, *Physics Reports* **2017**, 67, 1–52.
- (20) N.W. Ashcroft and N.D. Mermin. *Solid state Physics*. Saunders College, Philadelphia, PA 19105, *hwr international edition*, **1976**.
- (21) C.F. Bohren and D.R. Huffman. *Absorption and scattering of light by small particles* Wiley science paperback series. John Wiley & Sons, Inc., New York, **1983**.
- (22) T. Okamoto. *Near-field optics and surface plasmon polaritons*, volume 81 of *Topics in Applied Physics*. Pages 97-122, Springer, 2001.
- (23) S. Link, M. A. El-Sayed, *J. Phys. Chem. B* **1999**, 103, 4212-4217.
- (24) Mie, G., Beiträge zur optik trüber medien, speziell kolloidaler metallösungen. *Ann. Phys.* **1908**, 330, 377-445.
- (25) G. C. Papavassiliou, *Prog. Solid State Chem.* **1980**, 12, 185.
- (26) J. M. Luther, P. K. Jain, T. Ewers and A. P. Alivisatos, *Nat. Mater.*, 2011, 10, 361–366
- (27) S. D. Lounis, E. L. Runnerstrom. A. Bergerud, D. Nordlund, D. J. Milliron, *J. Am. Chem. Soc.*, **2014**, 136, 7110–7116.
- (28) U. Kreibig, L. Genzel, *Surf. Sci.*, **1985**, 156, 678.
- (29) S. Link, M. B. Mohamed, M. A. El-Sayed *J. Phys. Chem. B* **1999**, 103, 3073-3077.
- (30) R. Gans, Über die Form ultramikroskopischer Goldteilchen. *Annalen der Physik*, **1912**, 342, 881-900.
- (31) S. Link, M. A. El-Sayed, *J. Phys. Chem. B* **1999**, 103, 8410-8426.